Geophysical Research Letters

RESEARCH LETTER
10.1029/2023GL105246

# Comparing Local Versus Hemispheric Perspectives of Extreme Heat Events

**Senne Van Loon**[1,2] **and David W. J. Thompson**[2,3]

[1]Cooperative Institute for Research in the Atmosphere, Colorado State University, Fort Collins, CO, USA, [2]Department of Atmospheric Science, Colorado State University, Fort Collins, CO, USA, [3]School of Environmental Sciences, University of East Anglia, Norwich, UK

**Key Points:**

- Heat events expected less than once every century locally occur roughly once every 10 days somewhere in Northern Hemispheric midlatitudes
- Hemispheric incidence is underestimated by a factor 10 by normal statistics and strongly influenced by the shape of frequency distributions
- The large sample size of the hemispheric perspective clarifies the key role of mean temperature in driving observed trends in heat events

**Correspondence to:**

S. Van Loon,
Senne.Van_Loon@colostate.edu

**Citation:**

Van Loon, S., & Thompson, D. W. J. (2023). Comparing local versus hemispheric perspectives of extreme heat events. *Geophysical Research Letters*, *50*, e2023GL105246. https://doi.org/10.1029/2023GL105246

Received 28 JUN 2023
Accepted 4 DEC 2023

**Author Contributions:**

**Conceptualization:** Senne Van Loon, David W. J. Thompson
**Formal analysis:** Senne Van Loon
**Investigation:** Senne Van Loon, David W. J. Thompson
**Methodology:** Senne Van Loon, David W. J. Thompson
**Software:** Senne Van Loon
**Supervision:** David W. J. Thompson
**Visualization:** Senne Van Loon, David W. J. Thompson
**Writing – original draft:** Senne Van Loon, David W. J. Thompson
**Writing – review & editing:** Senne Van Loon, David W. J. Thompson



**Abstract** We compare insights provided by local and large-scale perspectives of extreme heat events in ERA5 near-surface temperature data. Heat waves where temperatures exceed four standard deviations about the climatological-mean are expected less than once a century locally but occur roughly once every 10 days somewhere in the Northern Hemisphere midlatitudes. The high frequency of occurrence indicated by the hemispheric perspective is not well represented by normal statistics because it strongly depends on the shapes of the local temperature distributions. The large effective sample size afforded by the hemispheric perspective provides robust evidence of trends in the frequency of occurrence of extreme heat events integrated over the Northern Hemisphere. It also confirms that trends in heat events summed over the hemisphere can be explained by changes in mean temperature alone.

**Plain Language Summary** Extreme events can be studied from local and large-scale perspectives. The two perspectives provide different insights into the likelihood of extreme events. For example, several notable recent heat waves in the Northern Hemisphere exceeded four standard deviations about the long-term climatology. Locally, such events are expected less than once every century. But based on high spatial resolution temperature data, such events occur somewhere in the Northern Hemisphere roughly once every 10 days. The increased likelihood of extreme heat events when summed over the hemisphere is not well represented by normal statistics because it is strongly dependent on the shapes of the temperature distributions. The large effective sample size afforded by the hemispheric perspective is important, as it provides a robust estimate of the influence of climate change on the frequency of occurrence of heat events. The hemispheric perspective confirms previous findings that long-term trends in extreme heat events summed over the Northern Hemisphere can be explained by recent increases in mean temperature.

## 1. Introduction

Extreme events are explored from both local and large-scale perspectives. The local perspective emphasizes case studies and the likelihood of a given event at a fixed location; the large-scale perspective emphasizes the incidence of such events integrated over large spatial scales.

Consider three recent notable heat events in the Northern Hemisphere: the June 2021 heat wave over the Pacific Northwest (e.g., Bartusek et al., 2022; Bercos-Hickey et al., 2022; Emerton et al., 2022; Heeter et al., 2023; Loikith & Kalashnikov, 2023; McKinnon & Simpson, 2022; Philip et al., 2022; Schumacher et al., 2022; Thompson et al., 2022; White et al., 2023), the July 2022 heat wave over the United Kingdom and Western Europe (e.g., Holley & Lee, 2022; Yule et al., 2023), and the July 2023 heatwave centered over the Mediterranean (https://climate.copernicus.eu/european-heatwave-july-2023-longer-term-context). From a local perspective, the likelihood of such events is very small: the return time of the 2021 Pacific Northwest heat wave has been estimated as anywhere from once in 200 years to once in 100,000 years (Bartusek et al., 2022; McKinnon & Simpson, 2022; Philip et al., 2022; White et al., 2023). From a large-scale perspective, the likelihood of such events increases rapidly as the size of the spatial domain—and thus the effective sample size—increases. The relationship between sample size and the incidence of heat events follows from an increase in the false discovery rate (Benjamini & Hochberg, 1995; Wilks, 2006) and is implicit in tests of the field significance (Livezey & Chen, 1983). The large-scale perspective has been increasingly used in analyses of heat events (e.g., Alexander et al., 2006; Domeisen et al., 2022; Fischer & Knutti, 2014; Fischer et al., 2021; Hansen et al., 2012; Perkins

et al., 2012; Power & Delage, 2019; Seneviratne et al., 2021; Tingley & Huybers, 2013; Vogel et al., 2019, 2020; Wang et al., 2021).

The purpose of this study is to contrast the local and hemispheric perspectives of heat events, and to use the latter to probe long term changes in heat events. We focus on heat events where the temperature exceeds four standard deviations above the climatological-mean during any season at any location in the Northern Hemisphere midlatitudes, and discuss the differences between using fixed or moving climatologies to define them. The key findings include the following: (a) Heat events expected less than once a century from a local perspective are observed somewhere in the Northern Hemisphere roughly once every 10 days in high spatial resolution surface temperature data. (b) The high frequency of occurrence of heat events when summed over the hemisphere is underestimated by at least an order of magnitude by normal statistics; it is highly dependent on the shapes of the frequency distributions of local temperature. And (c) the large sample size afforded by the hemispheric perspective confirms previous findings that the observed trends in heat events are due primarily to changes in mean temperature, as concluded in, for example, Simolo et al. (2011), Donat and Alexander (2012), Hansen et al. (2012), Rhines and Huybers (2013), McKinnon et al. (2016), Oliver et al. (2018), Seneviratne et al. (2021), McKinnon and Simpson (2022), Thompson et al. (2022), and Amaya et al. (2023).

## 2. Data and Methods

The analyses are based on daily mean, near-surface (2 m) temperatures ($T$) from the European Centre for Medium-Range Weather Forecasts Reanalysis v5 (ERA5, Hersbach et al., 2020, 2023). Daily mean values of $T$ were calculated from hourly mean values and are available on a 0.25° mesh. At 45° latitude, the 0.25° mesh is fine enough to capture heat events that span ∼20 km. The ERA5 2 m temperature data are not strictly speaking observations, but provide an excellent surrogate for assessing local temperature variability across the entire hemisphere (Sheridan et al., 2020).

There is a variety of different possible definitions for extreme heat events (e.g., Domeisen et al., 2022). Here we define extreme heat as days when temperatures exceed four standard deviations (+4s) about the long-term climatological mean. That is, days when temperatures are well outside the bounds of typical day-to-day variability. As discussed below, the preponderance of the frequency distributions of local temperatures closely follows the normal distribution, but local departures from the normal distribution contribute substantially to the probabilities of heat events. Unless otherwise specified, the climatology is defined with respect to the NOAA/WMO "US Climate Normal" 1991–2020 base period. The seasonal cycle is removed from the data as a function of grid point as follows: (a) We calculate the long-term 1991–2020 average of $T$ as a function of calendar day to form a 365-day climatology. (b) We apply a 31-day running mean filter to the 365-day climatology to minimize the effects of sampling variability on the climatology. (c) We subtract the resulting climatology from all years in the $T$ time series to form the anomalous temperature time series $T$*.

The standard deviation of $T$* during the 1991–2020 base period, denoted $s$, is found as a function of grid point as follows: (a) For each calendar day $i$, we extract all days in the $T$* time series that lie between calendar day $i - 15$ and calendar day $i + 15$. (b) We concatenate the 31 extracted days from each calendar year in the 1991–2020 base period into a single time series. (c) We calculate the standard deviation of the resulting concatenated time series. For example, in the case of the climatological standard deviation for 16 July, we calculate the standard deviation of all days in the $T$* time series that lie between 1 and 31 July and 1991–2020.

Skewness and kurtosis of the temperature anomalies are calculated at each grid point from the entire $T$* time series in the 1991–2020 base period. Although skewness and kurtosis are a function of season (Tamarin-Brodsky et al., 2020), we do not take seasonality into account here, as we do not differentiate between heat events in different seasons.

Trends in mean temperature are calculated using ERA5. To assess the reproducibility of the results based on temperature trends, we compare trends using ERA5 to those derived from the HadCRUT5 temperature data set (Morice et al., 2021). Differences in means between decades in ERA5 are very similar to those derived from HadCRUT5 (not shown).

We focus on all land and ocean areas in the Northern Hemisphere midlatitudes 30°N–70°N. We do not consider daily temperature extremes in the tropics, where much of the temperature variability is found on seasonal

timescales and is dominated by the El Niño Southern Oscillation. The diurnal cycle does not influence the results since we use daily mean data. Confidence levels are assessed by resampling the data with replacement (i.e., bootstrapping).

The +4s threshold provides a compromise between event amplitude and sample size. We also tested results for +3s and +5s; changing the threshold changes the number of events (by construction), but it does not alter the broad conclusions of the study.

The use of daily mean data at 0.25° horizontal resolution captures considerable temporal and spatial variability in the near-surface temperature field. The spatial degrees of freedom in the ERA5 near-surface temperature data are discussed in Section 3.3. We have checked key results using daily maximum temperature—which include variations on hourly timescales. The results closely mirror those based on daily mean data and do not notably alter the conclusions of the study (results not shown).

## 3. Results

### 3.1. Local Perspective

To provide context, we begin our analysis with a summary of three recent heat events: the June 2021 heat wave over the Pacific Northwest, the July 2022 heat wave over the United Kingdom and Western Europe, and the July 2023 heatwave centered over the Mediterranean. As indicated in Figure 1, all three events were marked by extreme heat over large spatial areas: temperature anomalies exceeded +4s over 1,070,000 km$^2$ of the Pacific Northwest on 29 June 2021, over 320,000 km$^2$ of Western Europe on 19 July 2022, and over 150,000 km$^2$ of the Mediterranean on 18 July 2023. At their peaks, the largest changes in daily mean temperatures exceeded 18°C, 14°C, and 12°C above the local 1991–2020 climatology, respectively.

From a local perspective, the likelihood of daily mean temperature exceeding +4s is very small. If daily mean temperatures are assumed to be normally distributed, then the likelihood of an extreme heat event exceeding +4s at any location is $3.2 \times 10^{-5} \approx 0.003\%$. Over land, where the decorrelation timescale of surface temperatures is on the order of a few days, the return time of +4s events is thus several centuries if the surface temperature is normally distributed.

However, surface temperatures exhibit notable departures from the normal distribution, and the shape of the temperature distribution has an important effect on the likelihood of extreme temperature events (e.g., Bjarke et al., 2022; Huybers et al., 2014; Lewis & King, 2017; Loikith & Neelin, 2015; McKinnon & Simpson, 2022; Ruff & Neelin, 2012; Sardeshmukh et al., 2015; Schär et al., 2004; Sippel et al., 2015; Sura, 2011; Sura & Perron, 2010). Figure 2a summarizes both theoretical and observed effects of skewness and kurtosis on the local incidence of heat events in 2 m temperature from ERA5 reanalysis. The figure is constructed as follows:

1. We calculate the skewness, kurtosis, and percentage of days when temperatures exceed +4s at each grid box in Northern Hemisphere midlatitudes, irrespective of seasonality. Shading in Figure 2a indicates the *local* percentage of days that exceed +4s as a function of skewness and kurtosis at the same location. White areas of the plot indicate grid boxes that have the indicated combinations of skewness and kurtosis, but for which there is no +4s event in the 1979–2022 period. Gray areas indicate combinations of skewness and kurtosis that are not found at any location.
2. We calculate the percentage of days when temperatures exceed +4s in random time series generated using a Pearson distribution with the observed skewness and kurtosis. The theoretical percentages are indicated by blue curves in Figure 2a.

The incidence of days exceeding +4s increases rapidly with both skewness and kurtosis. Grid points where temperatures are normally distributed exhibit percentages of ∼0.003%, as expected. But grid points where the skewness and kurtosis are large exhibit percentages as large as 0.2%, nearly two orders of magnitude larger than that predicted by the normal distribution. Skewness and kurtosis are closely related, but when combined, provide unique information on the shapes of frequency distributions. To first order, there is close correspondence between the predicted (blue curves in Figure 2a) and observed (shading in Figure 2a) incidence of days exceeding +4s. Figure 2b provides a companion analysis of the importance of the shapes of the frequency distributions for the *hemispheric* perspective, and is discussed in Section 3.3.

The physical processes that give rise to observed spatially varying patterns of skewness and kurtosis are considered elsewhere (e.g., Tamarin-Brodsky et al., 2020, 2022). But it is worth noting that many high values of

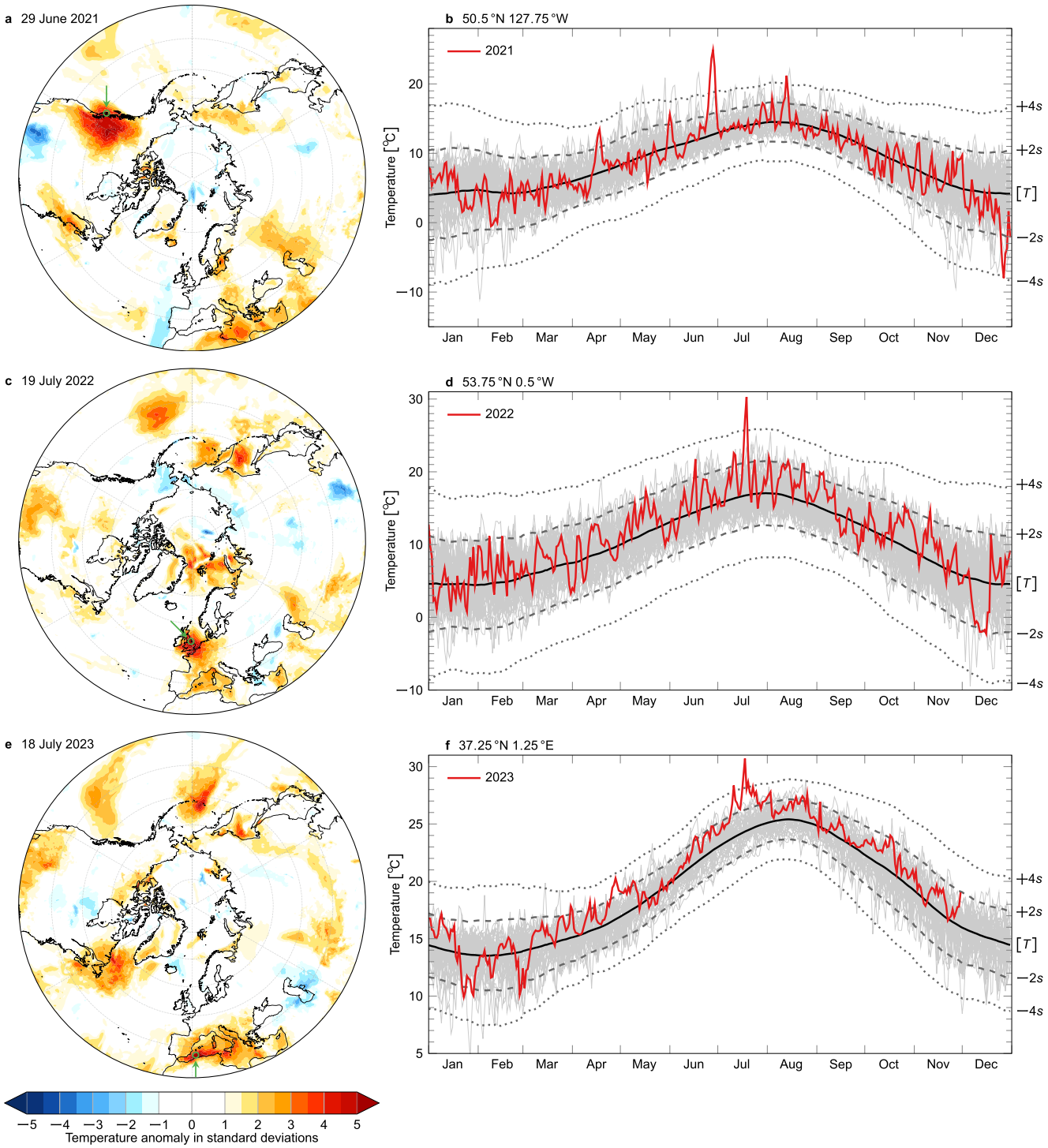


**Figure 1.** *Daily temperature for recent extreme heat events*. Panels (a, c, and e) show standardized temperature anomalies on 29 June 2021, 19 July 2022, and 18 July 2023. Panels (b, d, and f) show the daily averaged temperatures in 2021, 2022, and 2023 for the locations with the most extreme temperature on the days shown in panels (a, c, and e), respectively. Locations are indicated by green circles in the left column and centered at (50.5°N; 127.75°W), (53.75°N; 0.5°W), and (37.25°N; 1.25°E). The black lines in the right column show the long-term mean; the dashed and dotted gray lines indicate the 2s and 4s bands around the mean; the light gray lines are the daily averaged temperatures for all other years in the period 1979–2023.

skewness and kurtosis are found over coastal regions, and that comparisons between station data and ERA5 reveal some differences in such areas (Sheridan et al., 2020). Nevertheless, for this study, the key points in Figure 2a are that (a) large swaths of the hemisphere exhibit pronounced departures from normality; (b) the observed skewness

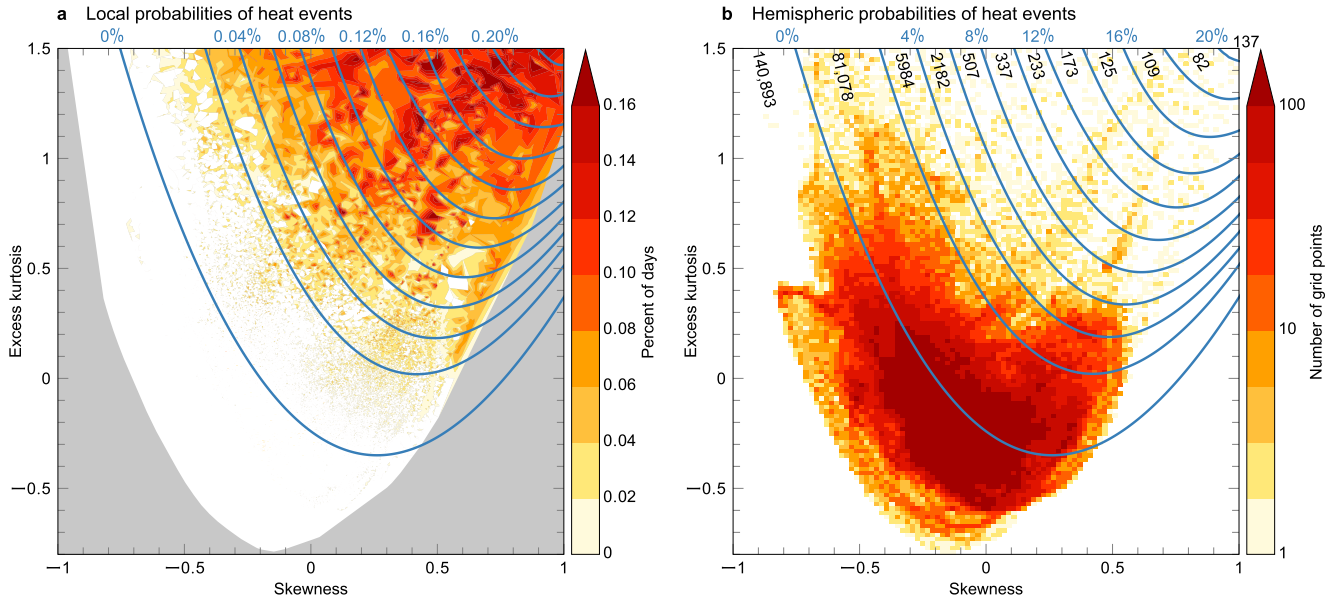


**Figure 2.** *Influence of skewness and kurtosis on local and hemispheric incidence of heat events.* (a) Contours: theoretical percent of days that temperature anomalies exceed +4s if they follow a Pearson distribution with skewness and kurtosis indicated on the axes. Shading: observed percent of days when local temperature anomalies exceeded +4s with respect to the 1991–2020 climatology. Results are calculated for all grid points in the Northern Hemisphere midlatitudes (30°N–70°N) and interpolated using Delaunay triangulation. Gray regions on the plot indicate values of skewness and kurtosis that are not found at any grid point. (b) Contours: theoretical percent of days that a temperature anomaly will exceed +4s in at least one of 100 independent time series if they follow a Pearson distribution with skewness and kurtosis indicated on the axes. Note that contours in panel (a) are for a single time series, and that contours in panel (b) are for 100 independent time series (there are roughly 100 spatial degrees of freedom in the Northern Hemisphere midlatitude temperature field). Shading: observed number of grid points in the Northern Hemisphere midlatitudes within a given skewness and kurtosis range using a bin size of 0.02 × 0.02. Black numbers indicate the total number of grid points that fall between the indicated probability contours.

and kurtosis lead to roughly an order of magnitude increase in the frequency of occurrence of extreme heat events relative to that predicted by normal statistics; and (c) the observed percent of days exceeding +4s matches that predicted by fitting Pearson distributions to the data.

Because +4s events are relatively rare on local scales—i.e., ranging from ∼0.003% for normally distributed data to ∼0.2% for highly skewed data—there are only a few occurrences that can be studied over relatively small spatial domains. Investigations of individual events are crucial for understanding their climate impacts and the underlying causal factors. However, the scarcity of samples, together with considerable internal variability on local scales, make it difficult to explore the effects of climate change on the incidence of heat waves when analyses are limited to specific locations.

### 3.2. Hemispheric-Scale Perspective

By construction, the hemispheric perspective of extreme heat events provides a much larger sample size than the local perspective, since the likelihood of daily mean temperature exceeding +4s anywhere in the hemisphere is a function of the spatial degrees of freedom in the surface temperature data. We discuss the spatial degrees of freedom in ERA5 surface temperature data in Section 3.3. Here, we explore the time-varying observed incidences of heat events summed over the Northern Hemisphere midlatitudes (30°N–70°N).

We consider three simple hemispheric-scale indices that quantify the time-varying incidence of extreme heat events. To separate out the dependence on spatial and temporal scales, we choose the following measures:

1. The percentage of days per decade during which at least one location in the Northern Hemisphere midlatitudes experiences a +4s heat event. We do not consider the timescale of individual events but simply the number of days when the +4s threshold is exceeded. The index is independent of temporal autocorrelations in the data because 3,650 days (i.e., the length of each sample used to estimate the percent of days) is much longer than the e-folding scale of daily mean, grid-point temperature.
2. The average number of days between a heat event of +4s occurring anywhere in the Northern Hemisphere midlatitudes. This statistic gives a sense of the typical number of days that elapse between successive +4s heat

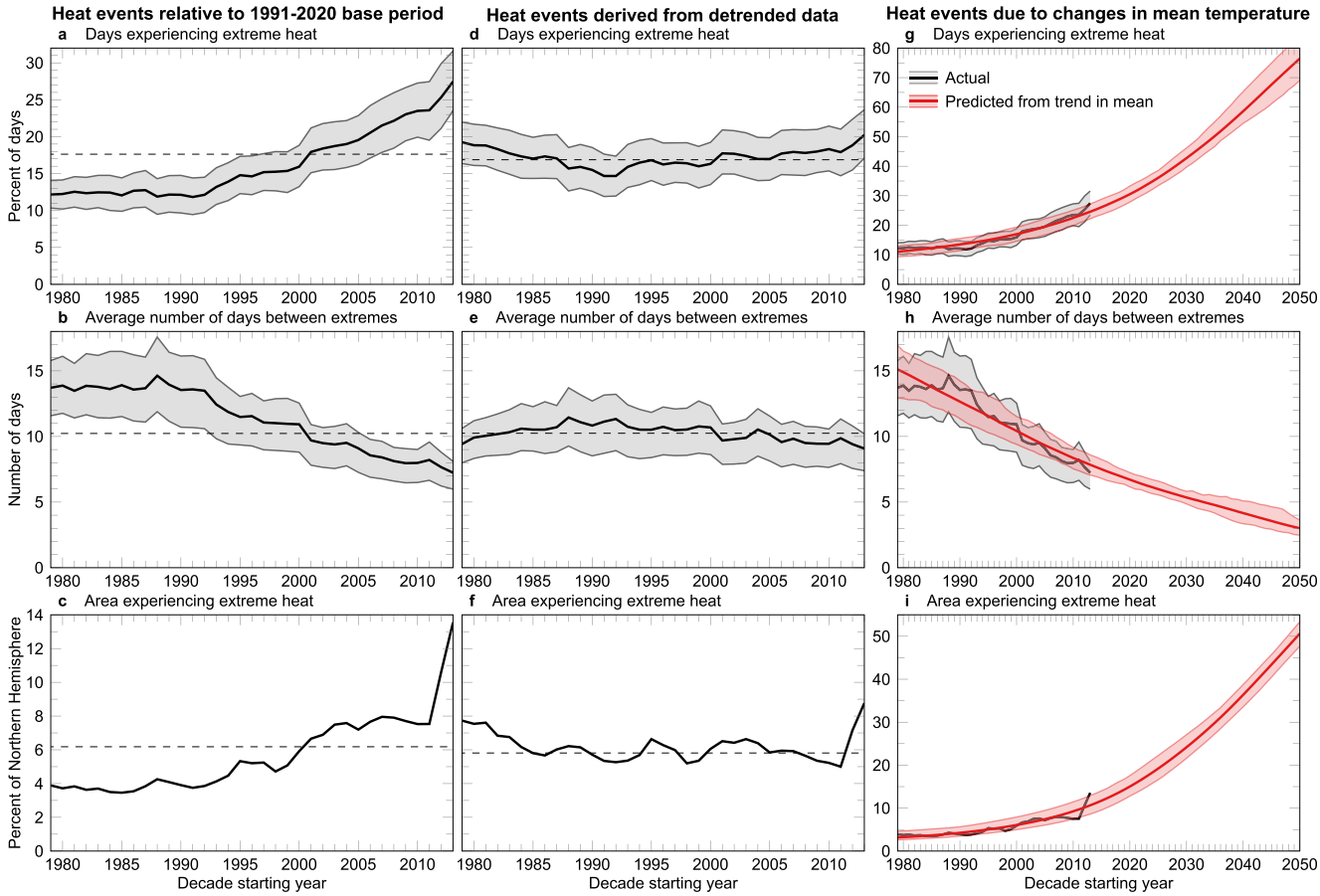


**Figure 3.** *Time evolution of the incidence of extreme heat events over the Northern Hemisphere midlatitudes*. Results are summed over successive decades, with the *x*-axes noting the starting year of each decade. Left column: (a) Percent of days in each decade that experienced an extreme heat event at least one location. (b) Average number of days between extreme heat events. (c) Percent of the Northern Hemisphere that experienced an extreme heat event on at least one day in each decade. Horizontal dashed lines denote the average over all decades in the base period 1991–2020. Gray shading show 95% confidence bounds computed by resampling with replacement. Middle column: Same as the left column, but for the incidence of heat waves based on detrended temperature anomalies. Right column: Black lines and gray shading are reproduced from the left column. Red lines indicate changes in extreme heat events found by allowing the mean temperature to change at each grid point but holding all other aspects of the temperature data fixed to a reference decade. Results for decades prior to 2013 are based on observed trends over 1979–2022; results for decades after 2013 show changes that will arise if the observed trends continue over the next four decades. The 95% confidence bounds are found by resampling the reference decade used in the analysis. See text for details.

events. It is related to the first statistic but is not necessarily identical since it is influenced by consecutive days exceeding +4s, and as such by temporal autocorrelation.

3. The fractional area of the hemisphere that experiences at least one +4s heat event in each decade. We do not consider repeat anomalies at the same location within a given decade. Because this index is integrated over a large domain, it is independent of the spatial autocorrelation structure of the data.

The results are shown in Figures 3a–3c. As noted in Section 2, the analyses are conducted with respect to the 1991–2020 climatology. The solid black lines show the results as a function of successive 10-year periods; the horizontal dashed lines show the results averaged over the base period 1991–2020. The gray shading in Figures 3a and 3b denotes the 95% confidence limits derived by resampling the data for individual months with replacement. Note that the confidence limits are a function of the total amplitude of the results and are thus slightly narrower when the amplitudes are smaller. Confidence limits are not calculated for the total area (Figure 3c) since—for this statistic—we do not count repeat events at the same location and thus resampling with replacement underestimates the amplitude of the results.

Averaged over the 1991–2020 base period (horizontal dashed lines), a temperature extreme exceeding +4s occurred somewhere in the Northern Hemisphere midlatitudes on 18% of all days (Figure 3a) with roughly 10 days between an event occurring anywhere in the midlatitudes (Figure 3b). That is, an event that is expected

less than once a century at a single location (assuming normal statistics and an e-folding timescale of a few days) occurs roughly once every 10 days when the likelihood is integrated over the Northern Hemisphere midlatitudes. Roughly 6% of the Northern Hemisphere midlatitudes experienced a +4s temperature anomaly per decade (Figure 3c).

All three measures of extreme temperature anomalies exhibit notable changes over the long-term period. As indicated by the confidence limits on Figures 3a and 3b, the changes are highly significant. The fraction of days marked by at least one +4s temperature anomaly in the Northern Hemisphere midlatitudes increased from 10% over the decade 1979–1988 to 30% over 2013–2022. The typical time between a +4s temperature anomaly occurring at any midlatitude location decreased from about two weeks over the decade 1979–1988 to one week over the decade 2013–2022. The fraction of the midlatitudes that experienced a +4s temperature anomaly increased from 4% over the decade 1979–1988 to 14% over 2013–2022. That is, the likelihood of any location experiencing an event that is +4s about the 1991–2020 climatology is almost three times higher today than it was in the 1980s.

### 3.3. Factors That Govern the Hemispheric-Scale Frequency of Occurrence

The results in Figure 3a indicate that a remarkable ∼18% of all days exhibit a +4s temperature event somewhere in Northern Hemisphere midlatitudes. The associated return time—which accounts for temporal autocorrelation in the data—is roughly 10 days. Here we consider the factors that give rise to such a large hemispheric frequency of occurrence: the effective spatial degrees of freedom and the shapes of the frequency distributions.

The first key factor is the spatial degrees of freedom in the data. One method for estimating spatial degrees of freedom involves solving for the eigenvalues of the temperature covariance matrix, and then solving for the effective degrees of freedom as $N^*_{\text{eff}} = \left(\sum_k f_k^2\right)^{-1}$, where $f_k$ is the fraction of variance explained by eigenvalue $k$, and the summation is performed over all eigenvalues (Bretherton et al., 1999). The downside of this method is that the spatial degrees of freedom are limited by the rank of the covariance matrix and thus the smallest dimension in the data. This is a potential issue if the number of temporal samples is smaller than the number of spatial samples, as is the case for high spatial resolution data.

An alternative method is to form an "effective" sample size by dividing the number of samples by the e-folding scale of the data (e.g., Bretherton et al., 1999; Leith, 1973). Here we adopt this method, but with two variations to account for the fact that we are working with two-dimensional data with nonstationary e-folding spatial scales. One, we calculate the number of grid boxes over which temporal correlation between adjacent grid boxes decreases to $e^{-1}$ in both the zonal and meridional directions, and form an e-folding area at each grid box as $A_j = X_j Y_j$. Here, $X_j$ and $Y_j$ denote the zonal and meridional e-folding distances in units of grid boxes and $j$ iterates all grid boxes. Two, we weight each grid box by its e-folding area and define $N_{\text{eff}}$ as the sum of the resulting weights, that is, $N_{\text{eff}} = \sum_j A_j^{-1}$. Weighting each grid box by $A_j^{-1}$ ensures that regions of fine-scale variability contribute more to the effective degrees of freedom than regions of relatively large-scale variability. The above calculation leads to roughly $N_{\text{eff}} \simeq 95$ spatial degrees of freedom in the 0.25° × 0.25° ERA5 surface temperature data over the 30°N–70°N region.

If we assume, say, 100 spatial degrees of freedom in the data, we expect to find temperatures exceeding +4s somewhere in the hemisphere on $1 - (1 - p_4)^{100} \simeq 0.3$ % of all days (where $p_4 = 3.2 \times 10^{-5}$ is the area under the normal curve for values greater than 4s). This is a factor of 60 lower than the ∼18% indicated in Figure 3a, and points to the importance of the second key factor that determines the hemispheric frequency of occurrence: the shapes of the temperature frequency distributions.

As discussed in Section 3.1, local temperatures exhibit well-known and notable departures from the normal distribution on the extremes of frequency distributions (e.g., Bjarke et al., 2022; Huybers et al., 2014; Lewis & King, 2017; Loikith & Neelin, 2015; McKinnon & Simpson, 2022; Ruff & Neelin, 2012; Sardeshmukh et al., 2015; Schär et al., 2004; Sippel et al., 2015; Sura, 2011; Sura & Perron, 2010; Tamarin-Brodsky et al., 2020). In the discussion of Figure 2a, we showed that the shapes of the temperature distributions significantly increase the incidence of heat events on the *local scale*; in Figure 2b, we consider their effects on the *hemispheric scale*:

1. For a given skewness and kurtosis, we generate 100 random time series (roughly the effective number of spatial degrees of freedom in the data) sampled from a Pearson distribution, and calculate the percent of days on which *any* of the random time series exceeds +4s. The analysis is repeated for all values of skewness and kurtosis and plotted as solid contours in Figure 2b.

2. We calculate the number of grid points in the ERA5 temperature data that fall within the range of skewness and kurtosis indicated on the axes and plot the results as shading. Note that the number of grid points is plotted using a log colorscale so that the results are visually apparent for a large range of grid points. The number of grid boxes that fall between the percentage curves is noted in black.

At skewness and kurtosis of zero, the percent of days in 100 randomly generated time series where at least one time series exceeds +4s is given from the normal distribution as $1-(1-p_4)^{100} \simeq 0.3\,\%$, as noted above. As shown in the contours in Figure 2b, this probability increases markedly as the skewness and kurtosis increase. Importantly, as indicated by the shading in Figure 2b, there are nearly 1,000 grid boxes in the ERA5 data that lie within the range where the observed skewness, kurtosis, and effective degrees of freedom should lead to temperatures exceeding +4s on at least ~10% of all days.

Hence, the observed skewness and kurtosis can increase the hemispheric incidence of extreme heat events by more than an order of magnitude relative to that expected from the normal distribution, as in the local perspective. At some grid points, the skewness and kurtosis likely underestimate the number of events on the tails of the distribution (e.g., Ruff & Neelin, 2012), which would further increase the predicted percentages. Despite the importance of the shapes of the distributions in determining the climatological-mean incidence of heat events, in the following section, we demonstrate that changes in the shapes of the frequency distributions of temperature play a *negligible* role in driving observed trends in extreme heat events.

### 3.4. Contribution of Changes in Mean Temperature

The significant trends in all three hemispheric measures of extreme events arise almost entirely from changes in the means of the local temperature frequency distributions, rather than their shapes. Figures 3d–3f show the same results as Figures 3a–3c, but in this case, we perform the analysis on data that have been detrended as a function of location and calendar day over the 1979–2022 period. Similar results are derived if, rather than detrend the data, we remove the 10-year running mean to account for non-stationarity in the long-term trend. The long-term *mean* of all three indices is comparable to that in Figures 3a–3c, but the long-term *trends* in all three indices are no longer significant. Hence, while changes in temperature variability and skewness may play a role in changes in extreme temperature anomalies over certain locations (Bjarke et al., 2022; Lewis & King, 2017; McKinnon & Simpson, 2022; McKinnon et al., 2016; Sardeshmukh et al., 2015; Schär et al., 2004; Schneider et al., 2015; Sippel et al., 2015; Tamarin-Brodsky et al., 2020), changes in mean temperature clearly account for the preponderance of the hemispherically integrated changes in heat events (e.g., Amaya et al., 2023; Donat & Alexander, 2012; Hansen et al., 2012; Oliver et al., 2018; Rhines & Huybers, 2013; Seneviratne et al., 2021; Simolo et al., 2011; Thompson et al., 2022).

How will continued increases in mean temperature influence the incidence of heat events? As noted above, from the perspective of an evolving climatology, we expect the incidence of heat events to remain largely fixed even as the Earth warms, as the shift in mean temperature is—by construction—accounted for in an evolving definition of the climatology. However, with respect to the 1991–2020 base climatology, continued increases in surface temperature will have an out-sized effect on events at the wings of the frequency distribution due to the exponential nature of the normal distribution.

We use the following methodology to estimate the changes in extreme heat events that will occur if the mean temperature continues to increase at the rate of the past four decades and heat events are considered with respect to the 1991–2020 base climatology. We form 35 decadal climatologies, one for every decade from 1979–1988 to 2013–2022 using the methodology outlined in Section 2. We denote these decadal climatologies with respect to the 1991–2020 base climatology $\overline{T}(j,c,d)$, where $j$ is the grid point, $c$ is calendar day, and $d$ is the decade used to construct the climatology. We compute the linear trend of $\overline{T}(j,c,d)$ as a function of decade, to define the spatially and seasonally varying trends in mean temperature per decade, $\Delta\overline{T}(j,c)$. We then form a series of 10-year-long synthetic anomalous temperature data sets by adding the temperature anomalies in the decade 1979–1988 to the trends in the temperature field given by $\Delta\overline{T}(j,c)\times\Delta t$, where $\Delta t$ is the difference between the start of the decade in question and 1979. For example, the synthetic data for the decade 2000–2009 is equal to the original data during the decade 1979–1988 plus $\Delta\overline{T}(j,c)\times(2000-1979)=\Delta\overline{T}(j,c)\times 21$. From 1979 to 2050, we synthesize 72 decades of data, where the mean is given by the linear trends in the data and the variability is given by the decade 1979–1988. We compute the three hemispheric measures, described in Section 3.2, using

these synthetic data sets. We then repeat the above calculation 35 times, varying the reference decade (and thus the variability of the synthetic data set) to account for all decades between 1979–1988 and 2013–2022. This method allows us to explore changes in extreme heat events in synthetic data where the local mean temperature changes from one decade to the next, but the shapes of the frequency distributions remain fixed to a given decade.

The results of the calculations are shown in Figures 3g–3i. The black lines and gray confidence limits are reproduced from Figures 3a–3c, but the aspect ratio is changed so that the observed period spans half the figure. The red lines and confidence limits show the corresponding changes predicted by the synthetic data sets described above, where the red shading indicates the range of results given by varying the reference decade to characterize variability about the mean. Consistent with the analysis in Figures 3d–3f, the changes in mean temperature account for effectively all the trends in extreme events in the existing record. The predicted changes in all three hemispherically integrated measures over the next few decades due entirely to continued changes in mean temperature are—as expected—very large.

## 4. Concluding Remarks

Extreme heat events can be explored from local and large-scale perspectives. The local perspective is the only way to perform individual case studies and assess risk at a fixed location; the large-scale perspective provides a large sample size for assessing the statistical behavior of extreme events over large spatial and time scales. Here we have highlighted different insights provided by the two perspectives.

As an example, we considered the incidence of heat events with similar amplitudes to the Pacific Northwest heat wave of 2021. From a local perspective, similar amplitude events are expected roughly once every century if temperature is normally distributed. However, when summed over the Northern Hemisphere midlatitudes in high-resolution surface temperature data, similar amplitude temperature anomalies arise roughly once every 10 days. The increased incidence afforded by the hemispheric-scale perspective is a well-known consequence of the increased spatial degrees of freedom in the data and is markedly influenced by the shapes of the local frequency distributions (Figure 2), see, for example, Ruff and Neelin (2012) and Bjarke et al. (2022). Considering both skewness and kurtosis of the local temperature distributions increases the expected hemispheric incidence of heat events by more than an order of magnitude relative to what is expected from normal statistics.

The larger sample size afforded by the hemispheric-scale perspective is useful for assessing the aggregate behavior of extreme heat events over the past few decades. Importantly, it confirms that the shapes of the local temperature distributions are key for the climatological incidence of heat events, but that changes in the shapes have not contributed to observed trends in the hemispheric incidence of heat events over the past 40 years. Rather, consistent with results reported in, for example, McKinnon and Simpson (2022), Seneviratne et al. (2021), and Thompson et al. (2022), the hemispheric perspective confirms that observed increases in heat events integrated over the Northern Hemisphere over the past 40 years are due primarily to changes in the mean temperature.

The key role of changes in the mean temperature suggests that recent increases in the hemispheric incidence of extreme events can be interpreted in two ways. If the increases are viewed with respect to a fixed climatology (e.g., the current WMO base-climatology of 1991–2020), then the incidence of extreme events has and will increase markedly with climate change (Figure 3 left and right columns). However, relative to a climatology that increases with global warming, changes in the incidence of extreme heat events are insignificant (Figure 3 middle column). Thus, the assessment of trends in heat waves depends highly on the definition of a heat wave, as discussed, for example, by Vogel et al. (2020) and Amaya et al. (2023). The choice of perspective depends on whether the climate impact of interest is susceptible to the absolute temperature—which would call for exploring the incidence of heat events from a fixed climatology—or is more susceptible to changes in temperature with respect to a time-evolving climatology.

## Data Availability Statement

All ERA5 data (Hersbach et al., 2020, 2023) is available at the Climate Data Store (C3S, 2023). HadCRUT5 data (Morice et al., 2021) is available from https://crudata.uea.ac.uk/cru/data//temperature/. All data analysis is done with Python 3.9 and Matlab R2022a. Figures are created in Python and PGF/Ti*k*Z.

**Acknowledgments**
We thank J. M. Wallace and an anonymous reviewer for constructive and helpful comments on the manuscript. We also thank N. Diffenbaugh for general comments on the paper. DWJT is funded by the NSF Climate and Large-Scale Dynamics Program AGS-2116186. SVL acknowledges the use of resources from the Cooperative Institute for Research in the Atmosphere at Colorado State University.

## References

Alexander, L. V., Zhang, X., Peterson, T. C., Caesar, J., Gleason, B., Klein Tank, A. M. G., et al. (2006). Global observed changes in daily climate extremes of temperature and precipitation. *Journal of Geophysical Research*, *111*(D5), D05109. https://doi.org/10.1029/2005JD006290

Amaya, D. J., Jacox, M. G., Fewings, M. R., Saba, V. S., Stuecker, M. F., Rykaczewski, R. R., et al. (2023). Marine heatwaves need clear definitions so coastal communities can adapt. *Nature*, *616*(7955), 29–32. https://doi.org/10.1038/d41586-023-00924-2

Bartusek, S., Kornhuber, K., & Ting, M. (2022). 2021 North American heatwave amplified by climate change-driven nonlinear interactions. *Nature Climate Change*, *12*(12), 1143–1150. https://doi.org/10.1038/s41558-022-01520-4

Benjamini, Y., & Hochberg, Y. (1995). Controlling the false discovery rate: A practical and powerful approach to multiple testing. *Journal of the Royal Statistical Society: Series B*, *57*(1), 289–300. https://doi.org/10.1111/j.2517-6161.1995.tb02031.x

Bercos-Hickey, E., O'Brien, T. A., Wehner, M. F., Zhang, L., Patricola, C. M., Huang, H., & Risser, M. D. (2022). Anthropogenic contributions to the 2021 Pacific Northwest heatwave. *Geophysical Research Letters*, *49*(23), e2022GL099396. https://doi.org/10.1029/2022GL099396

Bjarke, N., Barsugli, J., Hoerling, M., Quan, X.-W., & Livneh, B. (2022). When record breaking heat waves should not surprise: Skewness, heavy tails and implications for risk assessment (preprint). *Atmospheric Sciences*. https://doi.org/10.1002/essoar.10512706.1

Bretherton, C. S., Widmann, M., Dymnikov, V. P., Wallace, J. M., & Bladé, I. (1999). The effective number of spatial degrees of freedom of a time-varying field. *Journal of Climate*, *12*(7), 1990–2009. https://doi.org/10.1175/1520-0442(1999)012<1990:tenosd>2.0.co;2

C3S. (2023). *Copernicus climate change service, climate data Store, (2023): ERA5 hourly data on single levels from 1940 to present*. Copernicus Climate Change Service (C3S) Climate Data Store (CDS). Retrieved from https://cds.climate.copernicus.eu/

Domeisen, D. I. V., Eltahir, E. A. B., Fischer, E. M., Knutti, R., Perkins-Kirkpatrick, S. E., Schär, C., et al. (2022). Prediction and projection of heatwaves. *Nature Reviews Earth & Environment*, *4*(1), 36–50. https://doi.org/10.1038/s43017-022-00371-z

Donat, M. G., & Alexander, L. V. (2012). The shifting probability distribution of global daytime and night-time temperatures. *Geophysical Research Letters*, *39*(14), L14707. https://doi.org/10.1029/2012GL052459

Emerton, R., Brimicombe, C., Magnusson, L., Roberts, C., Di Napoli, C., Cloke, H. L., & Pappenberger, F. (2022). Predicting the unprecedented: Forecasting the June 2021 Pacific Northwest heatwave. *Weather*, *77*(8), 272–279. https://doi.org/10.1002/wea.4257

Fischer, E. M., & Knutti, R. (2014). Detection of spatially aggregated changes in temperature and precipitation extremes. *Geophysical Research Letters*, *41*(2), 547–554. https://doi.org/10.1002/2013GL058499

Fischer, E. M., Sippel, S., & Knutti, R. (2021). Increasing probability of record-shattering climate extremes. *Nature Climate Change*, *11*(8), 689–695. https://doi.org/10.1038/s41558-021-01092-9

Hansen, J., Sato, M., & Ruedy, R. (2012). Perception of climate change. *Proceedings of the National Academy of Sciences of the United States of America*, *109*(37), E2415–E2423. https://doi.org/10.1073/pnas.1205276109

Heeter, K. J., Harley, G. L., Abatzoglou, J. T., Anchukaitis, K. J., Cook, E. R., Coulthard, B. L., et al. (2023). Unprecedented 21st century heat across the Pacific Northwest of North America. *npj Climate and Atmospheric Science*, *6*(1), 5. https://doi.org/10.1038/s41612-023-00340-3

Hersbach, H., Bell, B., Berrisford, P., Biavati, G., Horányi, A., Muñoz-Sabater, J., et al. (2023). ERA5 hourly data on single levels from 1940 to present. *Copernicus Climate Change Service (C3S) Climate Data Store (CDS)*. https://doi.org/10.24381/cds.adbb2d47

Hersbach, H., Bell, B., Berrisford, P., Hirahara, S., Horányi, A., Muñoz-Sabater, J., et al. (2020). The ERA5 global reanalysis. *Quarterly Journal of the Royal Meteorological Society*, *146*(730), 1999–2049. https://doi.org/10.1002/qj.3803

Holley, D., & Lee, S. H. (2022). Forecasting extreme heat in the UK during July 2022. *Weather*, *77*(9), 320–321. https://doi.org/10.1002/wea.4290

Huybers, P., McKinnon, K. A., Rhines, A., & Tingley, M. (2014). U.S. daily temperatures: The meaning of extremes in the context of non-normality. *Journal of Climate*, *27*(19), 7368–7384. https://doi.org/10.1175/jcli-d-14-00216.1

Leith, C. E. (1973). The standard Error of time-average estimates of climatic means. *Journal of Applied Meteorology*, *12*(6), 1066–1069. https://doi.org/10.1175/1520-0450(1973)012<1066:tseota>2.0.co;2

Lewis, S. C., & King, A. D. (2017). Evolution of mean, variance and extremes in 21st century temperatures. *Weather and Climate Extremes*, *15*, 1–10. https://doi.org/10.1016/j.wace.2016.11.002

Livezey, R. E., & Chen, W. (1983). Statistical field significance and its determination by Monte Carlo techniques. *Monthly Weather Review*, *111*(1), 46–59. https://doi.org/10.1175/1520-0493(1983)111<0046:sfsaid>2.0.co;2

Loikith, P. C., & Kalashnikov, D. A. (2023). Meteorological analysis of the Pacific Northwest June 2021 heat wave. *Monthly Weather Review*, *151*(5), 1303–1319. https://doi.org/10.1175/MWR-D-22-0284.1

Loikith, P. C., & Neelin, J. D. (2015). Short-tailed temperature distributions over North America and implications for future changes in extremes. *Geophysical Research Letters*, *42*(20), 8577–8585. https://doi.org/10.1002/2015gl065602

McKinnon, K. A., Rhines, A., Tingley, M. P., & Huybers, P. (2016). The changing shape of Northern Hemisphere summer temperature distributions. *Journal of Geophysical Research: Atmospheres*, *121*(15), 8849–8868. https://doi.org/10.1002/2016JD025292

McKinnon, K. A., & Simpson, I. R. (2022). How unexpected was the 2021 Pacific Northwest heatwave? *Geophysical Research Letters*, *49*(18), e2022GL100380. https://doi.org/10.1029/2022GL100380

Morice, C. P., Kennedy, J. J., Rayner, N. A., Winn, J. P., Hogan, E., Killick, R. E., et al. (2021). An updated assessment of near-surface temperature change from 1850: The HadCRUT5 data set. *Journal of Geophysical Research: Atmospheres*, *126*(3), e2019JD032361. https://doi.org/10.1029/2019JD032361

Oliver, E. C. J., Donat, M. G., Burrows, M. T., Moore, P. J., Smale, D. A., Alexander, L. V., et al. (2018). Longer and more frequent marine heatwaves over the past century. *Nature Communications*, *9*(1), 1324. https://doi.org/10.1038/s41467-018-03732-9

Perkins, S. E., Alexander, L. V., & Nairn, J. R. (2012). Increasing frequency, intensity and duration of observed global heatwaves and warm spells. *Geophysical Research Letters*, *39*(20), L20714. https://doi.org/10.1029/2012GL053361

Philip, S. Y., Kew, S. F., Van Oldenborgh, G. J., Anslow, F. S., Seneviratne, S. I., Vautard, R., et al. (2022). Rapid attribution analysis of the extraordinary heat wave on the Pacific coast of the US and Canada in June 2021. *Earth System Dynamics*, *13*(4), 1689–1713. https://doi.org/10.5194/esd-13-1689-2022

Power, S. B., & Delage, F. P. D. (2019). Setting and smashing extreme temperature records over the coming century. *Nature Climate Change*, *9*(7), 529–534. https://doi.org/10.1038/s41558-019-0498-5

Rhines, A., & Huybers, P. (2013). Frequent summer temperature extremes reflect changes in the mean, not the variance. *Proceedings of the National Academy of Sciences*, *110*(7), E546. https://doi.org/10.1073/pnas.1218748110

Ruff, T. W., & Neelin, J. D. (2012). Long tails in regional surface temperature probability distributions with implications for extremes under global warming. *Geophysical Research Letters*, *39*(4), L04704. https://doi.org/10.1029/2011gl050610

Sardeshmukh, P. D., Compo, G. P., & Penland, C. (2015). Need for caution in interpreting extreme weather statistics. *Journal of Climate*, *28*(23), 9166–9187. https://doi.org/10.1175/JCLI-D-15-0020.1

Schär, C., Vidale, P. L., Lüthi, D., Frei, C., Häberli, C., Liniger, M. A., & Appenzeller, C. (2004). The role of increasing temperature variability in European summer heatwaves. *Nature*, *427*(6972), 332–336. https://doi.org/10.1038/nature02300

Schneider, T., Bischoff, T., & Płotka, H. (2015). Physics of changes in synoptic midlatitude temperature variability. *Journal of Climate*, *28*(6), 2312–2331. https://doi.org/10.1175/jcli-d-14-00632.1

Schumacher, D. L., Hauser, M., & Seneviratne, S. I. (2022). Drivers and mechanisms of the 2021 Pacific Northwest heatwave. *Earth's Future*, *10*(12),e2022EF002967. https://doi.org/10.1029/2022EF002967

Seneviratne, S., Zhang, X., Adnan, M., Badi, W., Dereczynski, C., Di Luca, A., et al. (2021). Weather and climate extreme events in a changing climate. In V. Masson-Delmotte, P. Zhai, A. Pirani, S. L. Connors, C. Péan, S. Berger, et al. (Eds.), *Climate change 2021: The physical science basis. Contribution of working group I to the sixth assessment report of the intergovernmental panel on climate change* (pp. 1513–1766). Cambridge University Press. https://doi.org/10.1017/9781009157896.013

Sheridan, S. C., Lee, C. C., & Smith, E. T. (2020). A comparison between station observations and reanalysis data in the identification of extreme temperature events. *Geophysical Research Letters*, *47*(15), e2020GL088120. https://doi.org/10.1029/2020GL088120

Simolo, C., Brunetti, M., Maugeri, M., & Nanni, T. (2011). Evolution of extreme temperatures in a warming climate. *Geophysical Research Letters*, *38*(16), L16701. https://doi.org/10.1029/2011GL048437

Sippel, S., Zscheischler, J., Heimann, M., Otto, F. E. L., Peters, J., & Mahecha, M. D. (2015). Quantifying changes in climate variability and extremes: Pitfalls and their overcoming. *Geophysical Research Letters*, *42*(22), 9990–9998. https://doi.org/10.1002/2015GL066307

Sura, P. (2011). A general perspective of extreme events in weather and climate. *Atmospheric Research*, *101*(1–2), 1–21. https://doi.org/10.1016/j.atmosres.2011.01.012

Sura, P., & Perron, M. (2010). Extreme events and the general circulation: Observations and stochastic model dynamics. *Journal of the Atmospheric Sciences*, *67*(9), 2785–2804. https://doi.org/10.1175/2010jas3369.1

Tamarin-Brodsky, T., Hodges, K., Hoskins, B. J., & Shepherd, T. G. (2020). Changes in Northern Hemisphere temperature variability shaped by regional warming patterns. *Nature Geoscience*, *13*(6), 414–421. https://doi.org/10.1038/s41561-020-0576-3

Tamarin-Brodsky, T., Hodges, K., Hoskins, B. J., & Shepherd, T. G. (2022). A simple model for interpreting temperature variability and its higher-order changes. *Journal of Climate*, *35*(1), 387–403. https://doi.org/10.1175/JCLI-D-21-0310.1

Thompson, V., Kennedy-Asser, A. T., Vosper, E., Lo, Y. T. E., Huntingford, C., Andrews, O., et al. (2022). The 2021 western North America heat wave among the most extreme events ever recorded globally. *Science Advances*, *8*(18), eabm6860. https://doi.org/10.1126/sciadv.abm6860

Tingley, M. P., & Huybers, P. (2013). Recent temperature extremes at high northern latitudes unprecedented in the past 600 years. *Nature*, *496*(7444), 201–205. https://doi.org/10.1038/nature11969

Vogel, M. M., Zscheischler, J., Fischer, E. M., & Seneviratne, S. I. (2020). Development of future heatwaves for different hazard thresholds. *Journal of Geophysical Research: Atmospheres*, *125*(9), e2019JD032070. https://doi.org/10.1029/2019JD032070

Vogel, M. M., Zscheischler, J., Wartenburger, R., Dee, D., & Seneviratne, S. I. (2019). Concurrent 2018 hot extremes across northern hemisphere due to human-induced climate change. *Earth's Future*, *7*(7), 692–703. https://doi.org/10.1029/2019EF001189

Wang, J., Li, C., Zwiers, F., Zhang, X., Li, G., Jiang, Z., et al. (2021). On the optimal design of field significance tests for changes in climate extremes. *Geophysical Research Letters*, *48*(9), e2021GL092831. https://doi.org/10.1029/2021GL092831

White, R. H., Anderson, S., Booth, J. F., Braich, G., Draeger, C., Fei, C., et al. (2023). The unprecedented Pacific Northwest heatwave of June 2021. *Nature Communications*, *14*(1), 727. https://doi.org/10.1038/s41467-023-36289-3

Wilks, D. S. (2006). On "field significance" and the false discovery rate. *Journal of Applied Meteorology and Climatology*, *45*(9), 1181–1189. https://doi.org/10.1175/JAM2404.1

Yule, E. L., Hegerl, G., Schurer, A., & Hawkins, E. (2023). Using early extremes to place the 2022 UK heat waves into historical context. *Atmospheric Science Letters*, *24*(7), e1159. https://doi.org/10.1002/asl.1159